

Structure and properties of the integer-spin frustrated antiferromagnet GeNi_2O_4

M. K. Crawford,¹ R. L. Harlow,¹ P. L. Lee,² Y. Zhang,² J. Hormadaly,³ R. Flippen,¹ Q. Huang,⁴ J. W. Lynn,⁴ R. Stevens,⁵ B. F. Woodfield,⁵ J. Boerio-Goates,⁵ and R. A. Fisher⁶

¹DuPont Co., Central Research and Development Department, E356/209, Wilmington, Delaware 19880-0356, USA

²Advanced Photon Source, Argonne National Laboratory, Argonne, Illinois 60439, USA

³Ben Gurion University of the Negev, Beer Sheeva, Israel

⁴NIST Center for Neutron Research, National Institute of Standards and Technology, Gaithersburg, Maryland 20899-8562, USA

⁵Department of Chemistry and Biochemistry, Brigham Young University, Provo, Utah 84602, USA

⁶Lawrence Berkeley National Laboratory, University of California, Berkeley, California 94720, USA

(Received 16 June 2003; published 31 December 2003)

We report the results of magnetic susceptibility, specific heat, synchrotron x-ray, and neutron powder diffraction measurements for the normal spinel GeNi_2O_4 , which becomes antiferromagnetic below a Néel temperature (T_N) of 12 K. The Néel transition occurs in two discrete steps, separated in temperature by 0.6 K. The total magnetic entropy evaluated from the specific heat data is only $\sim 1/2$ of the expected $2R \ln 3$ per mole of GeNi_2O_4 . The specific heat data also suggest the presence of both gapless and gapped excitations within the Néel state. GeNi_2O_4 remains cubic to temperatures well below T_N .

DOI: 10.1103/PhysRevB.68.220408

PACS number(s): 75.50.Ee, 75.25.+z, 75.40.-s, 75.50.-y

For some time there has been growing interest in the properties of strongly frustrated magnets. Spinel and pyrochlores are two of the most important crystal structures that are known to exhibit geometric magnetic frustration. In these materials there are three-dimensional networks of corner-sharing tetrahedra, a structural arrangement that leads to a high degree of magnetic frustration if the dominant nearest-neighbor interactions are antiferromagnetic. Depending upon the exact nature of the magnetic interactions, exotic ground states such as spin liquids¹ or spin ices² have been observed for rare earth ions on the pyrochlore lattice. Structural phase transitions, which have been interpreted to be three-dimensional analogs of spin-Peierls transitions, have also been observed³ in spinels with transition metal ions located on the geometrically frustrated B sublattice.

One interesting question that has not, to our knowledge, been addressed experimentally concerns the possible effect of spin statistics on the magnetic excitations in frustrated lattices. Several recent theoretical discussions^{4,5} suggest that the excitations of integer Heisenberg spins might in fact differ significantly from those of half-integer spins on the pyrochlore lattice. In order to address this issue we have been systematically investigating the magnetic and structural properties of spinels in which integer or half-integer-spin transition metal ions are located on the B sublattice. In this paper we describe the results for an integer-spin ($S=1$) frustrated magnet GeNi_2O_4 .

GeNi_2O_4 adopts the normal spinel crystal structure, with the magnetic Ni^{2+} ions located on the vertices of corner-sharing tetrahedra. Each Ni^{2+} ion is coordinated by a nearly regular octahedron of oxygen ions. The free Ni^{2+} ion has a 3F_4 ground state, which splits in an octahedral (cubic) crystal field to yield a ${}^3A_{2g}$ ground state, and several excited states located at much higher energies. Due to a combination of the actual trigonal crystal field at the spinel B site and second-order spin-orbit coupling between the higher crystal field states and the ground state, the triply degenerate ${}^3A_{2g}$ ground state will further split into two levels, a spin-singlet

and a doublet, separated by an energy on the order of a few cm^{-1} or less. The doublet is generally lower in energy.

In Fig. 1 we show the magnetic susceptibility⁶ of GeNi_2O_4 . A Curie-Weiss fit to the high temperature region of the inverse susceptibility yields a magnetic moment of $3.3\mu_B$ for the Ni^{2+} ions, and a Weiss constant of $\theta_w = -4.4$ K. This moment, somewhat larger than the spin only value of $2.83\mu_B$, leads to a Landé g factor of 2.33. The small negative value of the Weiss constant is consistent with the near-cancellation of nearest-neighbor and further-neighbor superexchange for Ni^{2+} ions on this lattice.

The data in Fig. 1 also show a magnetic transition near 12 K, in agreement with previous magnetic susceptibility and neutron powder diffraction measurements.⁷ The latter show that the magnetic order below this transition is antiferromagnetic. Upon closer examination by magnetic susceptibility (Fig. 1) and specific heat⁸ (Fig. 2) measurements, however, the Néel transition is seen to consist of two separate transitions, one at $T_{N_1} = 12.13$ K and the second at $T_{N_2} = 11.46$ K (in zero field). The transitions are not of the usual second-order lambda shape, instead rising more steeply for $T < T_N$ and falling less steeply for $T > T_N$, and in fact may be first order.

We have used neutron powder diffraction data, obtained at the NIST Center for Neutron Research, to verify the presence of a bulk two-step Néel transition. The intensity of the $(1/2, 1/2, 1/2)$ magnetic Bragg reflection shows a two-step behavior (Fig. 3), as do the $(3/2, 3/2, 3/2)$ and $(3/2, 3/2, 1/2)$ Bragg reflections (not shown). Our neutron powder diffraction data can be modeled with a simple collinear two-sublattice antiferromagnetic structure,⁷ in which spins in (111) sheets are aligned ferromagnetically. Refinement⁹ of our neutron diffraction data collected at $T = 1.4$ K, using a tetragonal magnetic unit cell with lattice parameters $a = \sqrt{2}a_{\text{cubic}} = 11.6237 \text{ \AA}$, $c = 2a_{\text{cubic}} = 16.4384 \text{ \AA}$, yields an ordered Ni^{2+} magnetic moment of $2.2\mu_B$, equal to the full moment expected for an $S=1$ ion with a Landé g factor of 2.33.

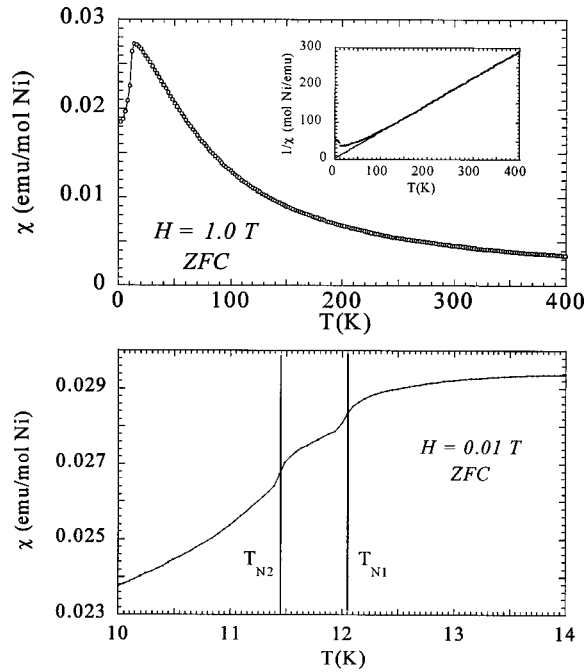


FIG. 1. (Top) The magnetic susceptibility of GeNi_2O_4 and (inset) the inverse magnetic susceptibility with a superimposed Curie-Weiss fit. The data were collected in a magnetic field of 1.0 T while warming, after cooling in zero field. (Bottom) Zero-field-cooled (0.01 T) magnetic susceptibility of GeNi_2O_4 , showing the two-step Néel transition.

Antiferromagnetic spin waves associated with the Ni^{2+} ordering in GeNi_2O_4 should be essentially isotropic, with the specific heat given by $C_{afsw} = B_{afsw} T^3$ at low T . However, we find that in order to adequately fit the heat capacity data below 4.5 K, it is necessary to add to the $B_{afsw} T^3$ term an additional term of the form $C_x = B_x T^n e^{-\Delta/T}$. This term represents a gapped excitation in the Néel state. The values of n and Δ which best fit the data are 0 and 11 K, respectively (Fig. 2). Although we currently have no definitive physical interpretation for this additional term in the heat capacity (for example, that is due to an anisotropy gap), our analysis of the heat capacity data suggests that a gapless spin-wave mode, characteristic of an isotropic antiferromagnet, coexists with a gapped mode in the Néel state of GeNi_2O_4 .

The total magnetic entropy S_{mag} extracted from the heat capacity measurements⁸ is only 56.5% of the $R \ln 3$ expected per mole of Ni^{2+} ions. At low temperatures, where neutron diffraction demonstrates the presence of long-range Néel order, we assume that $S_{mag} = 0$. The entropy up to T_{N1} , associated with destruction of long-range order, accounts for approximately half of the observed total. The balance, attributed to the destruction of short-range order, is observed above T_{N1} . The persistence of significant short-range order above 75 K is likely since the total magnetic entropy falls so short of the expected value. We have no definitive model at present for the form of this short-range order, although it is possible to postulate various spin clusters that can account for the missing entropy.

The presence of two magnetic transitions in GeNi_2O_4 ,

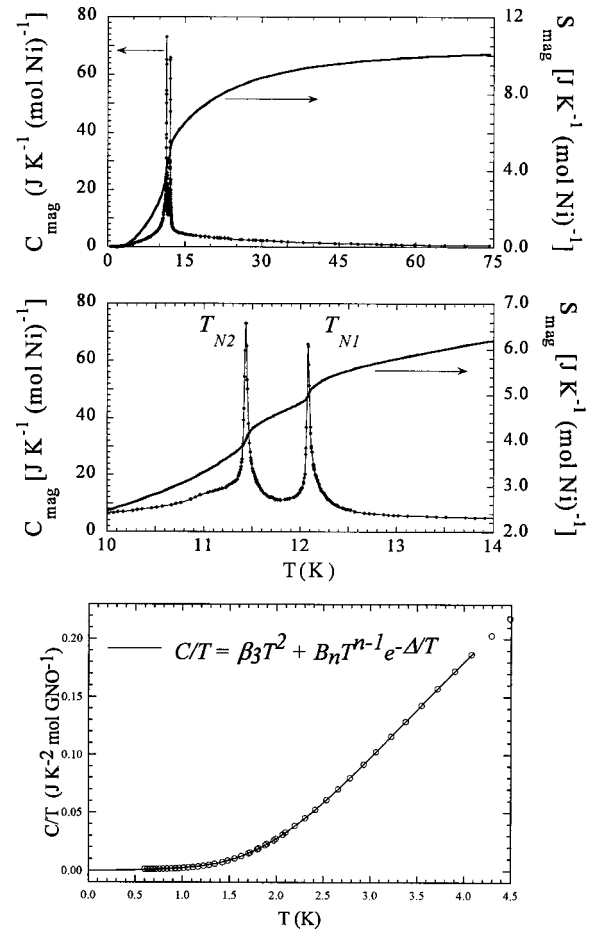


FIG. 2. (Top) The zero-field magnetic heat capacity and entropy for GeNi_2O_4 from 0.7 to 75 K. (Middle) Expanded view of the magnetic heat capacity showing the two-step Néel transition, and the magnetic entropy associated with the Néel transition. The entropies evolved at T_{N1} and T_{N2} are 2% and 3.6% of the $2R \ln 3$ expected per mole of GeNi_2O_4 . (bottom) C/T vs T for GeNi_2O_4 . The data (points) can be well fit (solid line) assuming the presence of three contributions: an isotropic three-dimensional gapless spin-wave and phonons (T^3 term), and a gapped magnetic excitation (exponential term; see the text and Ref. 8). The magnetic contribution to the T^3 term is about eight times larger than that due to phonons in this temperature range.

although interesting, is not unique.¹⁰ For example, CsNiCl_3 , a one-dimensional triangular Heisenberg antiferromagnet with a small easy-axis anisotropy parallel to the Ni^{2+} chain direction, also has a double Néel transition.^{10–12} The presence of two transitions is a result of the Ni^{2+} single-ion anisotropy. It is possible that a similar explanation holds for GeNi_2O_4 . Single crystal neutron diffraction studies will help to determine the origin of the two magnetic transitions in GeNi_2O_4 .

It is important to establish whether or not the crystal structure of GeNi_2O_4 remains cubic at T_N and below. Although our neutron diffraction data are consistent with cubic symmetry at temperatures well below T_N , we have also obtained much higher resolution synchrotron x-ray powder diffraction¹³ data in this temperature region. In Fig. 3, we

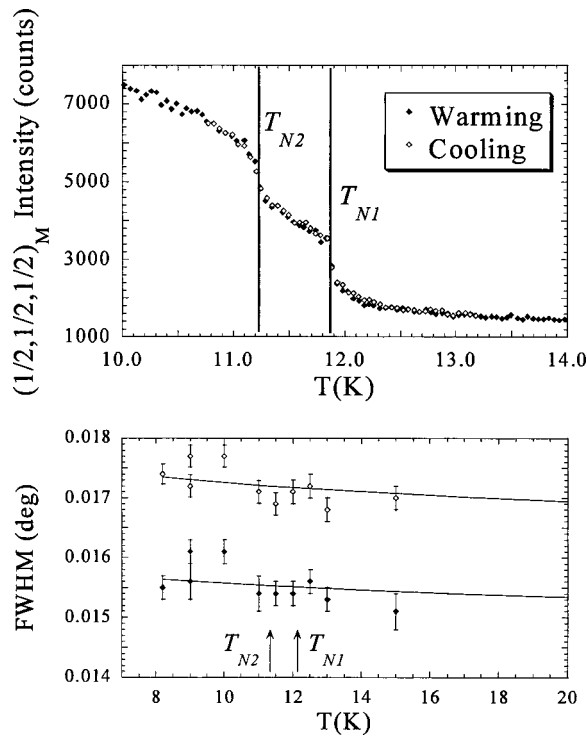


FIG. 3. (Top) Neutron powder diffraction measurement (BT-7 triple-axis spectrometer at NIST Center for Neutron Research) of the temperature dependence of the intensity of the $(1/2, 1/2, 1/2)$ magnetic Bragg reflection of GeNi_2O_4 , referenced to the cubic $Fd\bar{3}m$ unit cell, showing the double Néel transition. There is little thermal hysteresis in T_{N1} and T_{N2} . The a lattice parameter is $8.21967(8)$ Å at $T=13$ K. (bottom) The full width at half maximum intensity (FWHM) of the (444) (filled diamonds) and the (800) (open diamonds) nuclear Bragg reflections, as functions of temperature, measured by synchrotron x-ray powder diffraction. The locations of the two magnetic transitions, T_{N1} and T_{N2} , are also shown.

show the temperature dependence of the linewidths for the (444) and (800) Bragg reflections determined from the synchrotron x-ray diffraction data. *There is no discernible change in linewidth for the (800) or the (444) reflection¹⁴ directly associated with T_N .* This observation eliminates the possibility of either a tetragonal distortion (similar to that observed³ in, for example, ZnCr_2O_4), or a rhombohedral distortion (as observed¹⁵ in NiO), coupled to the appearance of Néel order in GeNi_2O_4 . The complete synchrotron x-ray diffraction pattern for GeNi_2O_4 at $T=7$ K is consistent with the cubic $Fd\bar{3}m$ symmetry present above T_N (Ref. 9).

The observation that GeNi_2O_4 remains cubic below T_N is in marked contrast with results for the transition metal oxide spinel ZnCr_2O_4 (Refs. 3 and 16). ZnCr_2O_4 undergoes a cubic-tetragonal structural phase transition at T_N . Such structural transitions have been described^{17,18} as three-dimensional analogs of the spin-Peierls transitions that occur in $S=1/2$ one-dimensional antiferromagnets. Furthermore, we have observed⁹ the appearance of tetragonal distortions in

two other spinels, GeCo_2O_4 ($S=3/2$, effective spin $1/2$ at low temperature) and ZnFe_2O_4 ($S=5/2$), each of which has half-integer-spin transition metal ions. In each of these cases, the structural transition is also closely associated with T_N , which suggests that distortions from cubic lattice symmetry generally occur at the Néel transitions in half-integer-spin magnetically frustrated spinels. In light of these observations for half-integer-spin systems, we suggest that the absence of a structural transition in GeNi_2O_4 may be a consequence of the integer-spin of the Ni^{2+} ion. In one-dimensional antiferromagnets, spin-Peierls transitions for spin-1 magnetic ions are prevented by the appearance of Haldane gaps, which render the chains rigid against dimerization.¹⁹ The observation of a gapped spin excitation in GeNi_2O_4 , and the absence of a structural transition, thus raises the question of whether a related phenomenon can also exist in a three-dimensional integer-spin *frustrated* lattice. This naturally leads us to consider the origin of the spin excitations that we have observed in the Néel state of GeNi_2O_4 .

Dispersionless spin-waves have been predicted²⁰ for the nearest-neighbor antiferromagnetic cubic pyrochlore lattice with classical vector spins, and evidence for such an excitation at 4.5 meV was reported³ for ZnCr_2O_4 . That excitation appeared abruptly at the coupled structural-magnetic transition to the Néel state, and was seen to coexist with a gapless ($\Delta < 1.5$ meV) three-dimensional spin-wave spectrum. The 4.5 meV excitation was later described as a cubic pyrochlore lattice Goldstone mode that had been shifted to finite frequency by the tetragonal lattice distortion¹⁸ in ZnCr_2O_4 .

In contrast, the gapped excitation in GeNi_2O_4 , which also coexists with gapless three-dimensional spin-waves, is a property of the Néel state *in the cubic structure*, and thus clearly requires a different explanation. Simple arguments²¹ suggest that valence bond solid ground states, which do not break lattice translational symmetry, can only be realized when $(2S/z) = \text{integer}$, where z is the number of nearest-neighbor spins of the magnetic ion. For GeNi_2O_4 , $z=6$ and $S=1$, so that condition is not fulfilled. In any case, the fact that integer spin GeNi_2O_4 does not undergo a structural phase transition, whereas several half-integer spin systems do, suggests there might be a connection between these phenomena. Additional experimental studies of the magnetic excitations in single crystal GeNi_2O_4 , and other integer-spin and half-integer-spin frustrated magnets, by inelastic neutron scattering techniques should provide insight into this possible relationship.

The authors acknowledge E.M. McCarron, R.J. Smalley, and T. Borecki for help with sample preparation. We would also like to thank Ian Affleck (Boston University), John Goodenough (University of Texas, Austin), and David Cox (Brookhaven National Laboratory) for helpful discussions concerning the results described in this paper. Use of the Advanced Photon Source was supported by the U.S. Department of Energy, Office of Science, Office of Basic Energy Sciences, under Contract No. W-31-109-ENG-38.

- ¹J.S. Gardner *et al.*, Phys. Rev. Lett. **82**, 1012 (1999).
- ²S.T. Bramwell and M.J.P. Gingras, Science **294**, 1495 (2001), and references therein.
- ³S.-H. Lee, C. Broholm, T.H. Kim, W. Ratcliff, and S.-W. Cheong, Phys. Rev. Lett. **84**, 3718 (2000).
- ⁴A. Koga and N. Kawakami, Phys. Rev. B **63**, 144432 (2001).
- ⁵Y. Yamashita, K. Ueda, and M. Sigrist, J. Phys.: Condens. Matter **13**, L961 (2001).
- ⁶Samples of GeNi_2O_4 were synthesized by standard solid-state techniques. Starting materials (GeO_2 and NiO) were reacted at 1200°C in an O_2 atmosphere for 24 h, ground, and fired again under the same conditions. X-ray and neutron diffraction data show the resulting material to be the normal spinel GeNi_2O_4 with less than 1% cation inversion, and any impurities were present at less than 0.5 weight percent. Magnetic susceptibility data were measured using a Quantum Design MPMS-7 superconducting quantum interference device magnetometer.
- ⁷E.F. Bertaut *et al.*, J. Phys. (France) **25**, 516 (1964).
- ⁸Heat capacity data were taken on two calorimeters and details of the measurements will be published elsewhere [R. Stevens *et al.*, J. Chem. Thermodyn. (to be published)]. The magnetic specific heat, C_{mag} , has been obtained in two independent procedures. In the first method, a set of Einstein and Debye functions were fit to the measured C for $T > 100$ K. The extrapolation of this expression to low temperatures was taken as C_{lat} , and C_{mag} determined from $C - C_{lat}$. The integral $\int [C_{mag}/T]dT$ from 0 to T yields the magnetic entropy, S_{mag} . In the second method, C_{mag} was obtained from a two-step analysis of the data for $T < T_{N_2}$ and $T > T_{N_1}$. An excellent representation of the data for $T \leq 4$ K is obtained using a non linear, least-squares procedure with the expression $C = \beta_3 T^3 + B_x T^n e^{-\Delta/T}$, where $\beta_3 = (B_3 + B_{afsw})$ and B_3 and B_{afsw} represent the phonon and spin-wave contributions, respectively. The parameters obtained by nonlinear regression techniques are $\beta_3 = 2.198 \times 10^{-3} \text{ J K}^{-4} \text{ mol}^{-1}$, $B_x = 9.03 \text{ J K}^{-1} \text{ mol}^{-1}$, $n = 0.1$, and $\Delta = 11.0$ K for one mole of GeNi_2O_4 . [A plot of $\ln(C - \beta_3 T^3)$ vs $1/T$ is linear to ~ 6 K.] Above T_{N_1} the fitting expression is: $C = \sum D_m/T^m + \sum B_n T^n$, where $\sum D_m/T^m$ ($m = 2-4$) is a semi-empirical representation of the short-range magnetic order and $\sum B_n T^n$ ($n = 3-11$, n odd) is the harmonic-lattice approximation, C_{lat} . From $T = 14-75$ K the fit yields $B_3 = 2.38 \times 10^{-4} \text{ J K}^{-4} (\text{mol GeNi}_2\text{O}_4)^{-1}$ with $\Theta_D = 386$ K. Combining B_3 and β_3 , the coefficient B_{afsw} expressed per mole of Ni^{2+} ion is $0.98 \times 10^{-3} \text{ J K}^{-4} \text{ mol}^{-1}$. The exchange constant can be estimated: $J = R/[2S(B_{afsw}/c_a R)^{1/3}] = 5$ K per mole Ni^{2+} , where $S = 1$ is the spin in the ground state and the constant $c_a = 0.113$ for cubic symmetry. The magnetic entropy is obtained as the sum of $\int [(C - C_{lat})/T]dT$ from $0-75$ K, and $\int [(D_2/T^3 + D_3/T^4 + D_4/T^5)]dT$ from 75 K to ∞ . The magnetic entropies obtained using these two different methods for modeling the lattice contribution were nearly identical.
- ⁹Q. Huang, J. W. Lynn, M. K. Crawford, R. L. Harlow, R.B. Flippen, and J. Hormadaly, *Proceedings of Ninth International Conference on Composites Engineering*, San Diego, CA, 2002, pp. 305 and 306; M.K. Crawford *et al.* (unpublished).
- ¹⁰M.F. Collins and O.A. Petrenko, Can. J. Phys. **75**, 605 (1997).
- ¹¹W.B. Yelon and D.E. Cox, Phys. Rev. B **7**, 2024 (1973).
- ¹²H. Kadowaki, K. Ubukoshi, and K. Hirakawa, J. Phys. Soc. Jpn. **56**, 751 (1987).
- ¹³Synchrotron x-ray powder diffraction data were collected on beamline 1-BM of X-Ray Operation and Research at the Advanced Photon Source, Argonne National Laboratory. The x-ray wavelength was $0.619347(23) \text{ \AA}$.
- ¹⁴A tetragonal distortion would split the (800), but not the (444), Bragg reflection. A rhombohedral distortion would split the (444), but not the (800), Bragg reflection.
- ¹⁵W.L. Roth, Phys. Rev. **110**, 1333 (1958).
- ¹⁶Y. Ueda, N. Fujiwara, and H. Yasuoka, J. Phys. Soc. Jpn. **66**, 778 (1997).
- ¹⁷Y. Yamashita and K. Ueda, Phys. Rev. Lett. **85**, 4960 (2000).
- ¹⁸O. Tchernyshyov, R. Moessner, and S.L. Sondhi, Phys. Rev. Lett. **88**, 067203 (2002).
- ¹⁹F.D.M. Haldane, J. Appl. Phys. **57**, 3359 (1985).
- ²⁰J.N. Reimers, A.J. Berlinsky, and A.-C. Shi, Phys. Rev. B **43**, 865 (1991).
- ²¹I. Affleck, T. Kennedy, E.H. Lieb, and H. Tasaki, Phys. Rev. Lett. **59**, 799 (1987).